Latin American Journal of Solids and Structures
www.lajss.org

Viscoelastic Relaxation Modulus Characterization Using Prony Series

Abstract

The mechanical behavior of viscoelastic materials is influenced, among other factors, by parameters like time and temperature. The present paper proposes a methodology for a thermorheologically and piezorheologically simple characterization of viscoelastic materials in the time domain based on experimental data using Prony Series and a mixed optimization technique based on Genetic Algorithms and Nonlinear Programming. The text discusses the influence of pressure and temperature on the mechanical behavior of those materials. The results are compared to experimental data in order to validate the methodology. The final results are very promising and the methodology proves to be effective in the identification of viscoelastic materials.

Keywords

Viscoelasticity, material characterization, Prony Series, Wiechert model, optimization.

Juliana E. Lopes Pacheco [a]
Carlos Alberto Bavastri [b]
Jucélio Tomás Pereira [b,*]

[a] Programa de Pós-graduação em Engenharia Mecânica, Universidade Federal do Paraná.
[b] Departamento de Engenharia Mecânica, Universidade Federal do Paraná, Curitiba, PR – Brasil.
[*] Author's e-mail: jucelio.tomas@ufpr.br

http://dx.doi.org/10.1590/1679-78251412

Received 18.06.2014
In revised form 18.09.2014
Accepted 18.10.2014
Available online 13.10.2014

1 INTRODUCTION

Polymers are materials that have increasingly been used in engineering projects mainly due to their versatility as well as their mechanical resistance. However, the study of their behavior, when submitted to mechanical loads, is still being developed, due to its complex molecular structure, which molds mechanical properties that change according to time and temperature.

In order to predict the mechanical behavior of such material, some methods have been developed - starting from a few characteristic material parameters – aiming at determining the results of different loading application throughout time and under temperature change effects, inherent to the use of structural components using viscoelastic materials (VEMs).

The mechanical behavior model of VEMs could be represented by springs and dampers in parallel or in series, as seen in the models by Maxwell and Kelvin/Voigt, respectively, also known as

'integer derivative models' (Brinson & Brinson, 2008). Another approach is given through models that employ a fractional derivative concept (Mainardi, 2010). For both cases, these material characterizations could be performed in frequency and time domains. However, these models prove to be defective as a way of representing the dynamic characteristics of most materials used in engineering in a wide spectrum of temperature and time/frequency.

A study comparing molecular theories that describe VEMs behavior and models based on fractional derivatives was performed by Bagley & Torvik (1983). Their work demonstrated that, from a reduced number of parameters, it is possible to predict with some precision the dynamic behavior of those materials. Using a fractional derivative model containing four or five parameters, Pritz (1996) has determined the characteristics of dynamic module and material loss factor of VEMs in the frequency domain. Also utilizing fractional calculation models, Lopes et al. (2004) used a methodology based on an inverse problem to characterize those materials. Thus, using the transmissibility model of a simple system composed by VEM as a resilient element and nonlinear optimization techniques, it was possible to characterize rheologically simple materials by a global adjustment of all curves measured at different temperatures. In the study by Lima et al. (2004), a methodology was established to perform the modeling in finite beam elements and rectangular plaques with a VEM layer, in order to attenuate the effect of vibration on structures by using the GHM model. Therefore, through numerical simulations, the answer in frequency functions was obtained, modal properties were calculated and finally compared to experimental data obtained from vibration tests carried out in laboratory. Another technique recently developed to determine the mechanical properties of VEMs is nanoindentation. In one of those applications, Huang et al. (2004) used nanoindentation with a spherical indentator to measure the flexibility modulus of polymethylmetacrilate and polycarbonate. In order to validate the results of calculations from nanoindentation tests, the same materials were also tested by using a dynamic mechanical analysis.

Prony Series were used by Park & Schapery (1999) in an attempt to apply an efficient numerical method in the time domain to relate relaxation and creep functions of VEMs, which were tested using experimental data from a few polymeric materials. A method for determining the Prony Series coefficients of a viscoelastic relaxation modulus was developed by Chen (2000) using load versus time data for different sequences of load ratio adjusted to the convolution integrals of tested materials. In temperatures above glass transition, components exhibit a more pronounced viscoelastic behavior. In a study presented by Hu et al. (2006), a tensile relaxation test was used to characterize the viscoelasticity of an epoxy component by determining the material relaxation modulus as a function of time. Beake (2006) also used nanoindentation to investigate the creep behavior of semicrystalline and amorphous polymers. Experimental data - for the first twenty seconds of load - were adapted to a logarithmic equation that represents the fractionate increase of depth in penetration during creep and, by adjusting creep data, it was possible to predict the extension and creep ratio for load ratio and maximum load. Two alternative approaches for estimate viscoelastic material functions under random excitation were proposed and analyzed by Sorvari & Malinen (2007). In the first one, Boltzmann's superposition principle and Tikhonov's regularization were used in a linear equation system. Then, the integral was transformed into a recursive expression using a Prony Series based representation of viscoelastic material functions, in which an optimization technique based on gradients was also applied. Results were compared in order to validate the proposed nu-

merical method. Felhös et al. (2008) have determined the viscoelastic mechanical properties of EPDM (ethylene propylene diene monomer) rubber through a dynamic mechanical thermal analysis. These authors used a fifteen-term Maxwell's generalized model to describe the material behavior, the frictional aspect of which was tested in a rolling ball on a plate-like device. The rolling test was simulated by FEM using mechanical VEM properties and the calculated results proved to be fairly in accordance with the experimental results. In another study, Sorvari & Hämäläinen (2010) evaluated conventional semi-analytic and implicit Runge-Kutta numerical methods both analytically and numerically in order to solve integral models of linear viscoelasticity using Prony Series.

During VEMs characterization process, the influence of temperature variation on the behavior of those materials becomes clear. A material can be defined as thermorheologically simple when all relaxation times are affected by temperature in the same way, thus allowing the application of the Time-Temperature Superposition Principle (TTSP) (Leaderman, 1943; Schwarzl & Staverman, 1952). When applying TTSP to a thermorheologically simple material, master curves emerge using a reduced time variable or shift factor to comprise a wider time range of data from a given material function (Ferry, 1980). Master curves from a relaxation modulus logarithm versus a time logarithm were built by Tobolsky (1956) from experimental data for a few polymers in different temperatures and superposed through a horizontal shift along the time logarithm axis. Chae et al. (2010) performed tensile relaxation experiments in polymeric components in the time domain in order to determine the relaxation modulus master curve with Prony Series application. These authors used the technique developed by Williams, Landel and Ferry (1955), in which shift factors can be determined graphically or by using the experimentally based equation, also known as WLF equation. This method uses the ratio α_T - or shift factor - of all relaxation times at temperature T, compared to a reference temperature value Ts, in order to determine the relation between temperature and polymer characteristics. By using WLF equation and TTSP, Li et al. (2007) researched the dependence on temperature and fatigue damage tensile levels on polymethilmetacrylate, which was tested in different temperature conditions and tensile creep, resulting in the master curve for that material.

Another factor that exerts some influence on VEMs behavior is hydrostatic pressure. Like thermorheology, there is piezorheology, which determinates the influence of pressure in VEMs behavior. In order to perform the pressure superposition throughout time, the material must be piezorheologically simple, in other words, all relaxation times must be affected by pressure in the same way, allowing the calculation of a shift factor (Ferry, 1980). O'Reilly (1962) studied the effect of pressure in polyvinyl acetate behavior in the glass transition temperature region, Tg, by using dielectric and volumetric measurement techniques. Subsequently, this author developed a shift factor that considers the effect of pressure - α_P - which contains an exponential relation between a characteristic material Constant and the pressure applied to the material. A comparison of shift factor models that evaluate pressure influence on the mechanical properties of materials was performed by Tschoegl et al. (2002). Among these models, Ferry-Stratton's model (FS) applies to low pressure ranges - around 10 MPa - because it does not take into account the dependence of the compressibility factor on pressure. However, models like O'Reilly's (OR) and Kovacs-Tait's (KT) incorporate an inverse dependence of the compressibility factor on pressure.

The present work proposes a methodology for the characterization of VEMs from tensile versus strain experimental data for different strain ratio. This methodology is best described in Pacheco

(2013). The proposed model is based on Prony Series and the adjustment between experimentally obtained curves and their numerical equivalents - in order to identify the material - is performed through hybrid optimization techniques.

2 THEORETICAL CONCEPTS AND MATHEMATICAL FORMULATION

2.1 Constitutive VEM models

VEMs are materials whose mechanical behavior is strongly dependent on speed application of loads at constant temperature. A material can be considered as 'linear viscoelastic' when its strain and strain rate are infinitesimal, and the stress-strain relation can be expressed by linear differential equations with constant coefficients. In linear VEMs, the constitutive relations can be posed by hereditary relations that are expressed by the linear viscoelasticity superposition principle and use the relaxation and creep modulus function.

Starting from Maxwell's Generalized Model and adding one more spring term leads to a model known as Wiechert model (Brinson & Brinson, 2008), according to Figure 1. This model could be represented by the relaxation modulus function $E(t)$ as follows (Christensen, 1971; Ferry, 1980)

$$E\left(t\right) = E_{\infty} + \sum_{q=1}^{TN} E_q e^{-\frac{t}{\tau_q}}, \tag{1}$$

where E_{∞} is the equilibrium modulus, and E_q and τ_q are the elastic components and relaxation time associated to the *q-th* $(1 \leq q \leq TN)$ Maxwell model component. In this case, TN is the total number of Prony Series terms. This relaxation function, which presents the sum of a series of exponential terms, could be interpreted as a mechanical element model like the one in Figure 1, also known as Prony Series.

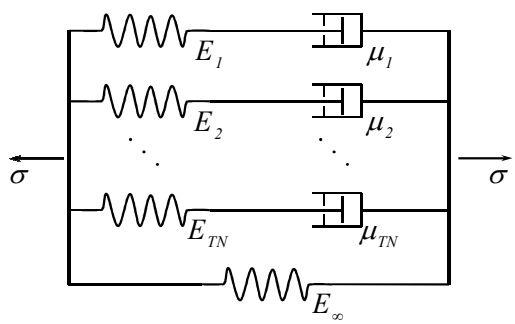

Figure 1: Wiechert material model.

Starting from Eq. (1), it yields that, for t = 0,

$$E\left(t = 0\right) = E_0 = E_{\infty} + \sum_{q=1}^{TN} E_q > 0, \tag{2}$$

where E_0 is the instantaneous relaxation modulus. Taking the limit to a very elevated time yields

$$\lim_{t\to\infty} E\left(t\right) = E_{\infty} \geq 0\,. \tag{3}$$

In this case, E_{∞} represents the material equilibrium modulus.

Considering a historical account of uniaxial strain - $\varepsilon(t)$ - the tensile $\sigma(t)$ can be obtained applying the hereditary integral (Flügge, 1975) as

$$\sigma\left(t\right) = E_{\infty}\varepsilon\left(0\right) + \int_{0}^{t} E\left(t-\tau\right)\frac{d\varepsilon\left(\tau\right)}{d\tau}d\tau\,, \tag{4}$$

where $\varepsilon(0)$ is the accumulated strain up to the initial instant (t = 0).

2.2 Identification Process Formulation in the Time Domain

In the present work, the identification process of mechanical properties of a VEM in the time domain considering the Wiechert model uses a family of experimental data obtained through uniaxial traction tests performed according to norm ISO 527/1B (ISO, 2012), with a constant strain rate. Thus,

$$\frac{d\varepsilon}{dt} = \dot{\varepsilon} = \text{constant for every time t}\,. \tag{5}$$

Considering this special case and a null initial strain, a reduced expression relating stress to historical strain can be obtained as follows

$$\sigma\left(t\right) = \dot{\varepsilon}\int_{0}^{t} E\left(t-\tau\right)d\tau\,. \tag{6}$$

Thus, the stress obtained from the Prony Series model (denoted by σ^{Prony}) can be expressed as

$$\sigma^{Prony} = \sigma^{Prony}\left(E_{\infty}, E_q, \dot{\varepsilon}, t\right) = \dot{\varepsilon}\sum_{q=1}^{TN} E_q \int_{0}^{t} e^{-\frac{(t-\tau)}{\tau_q}}\,d\tau\,. \tag{7}$$

A graphic visualization of the stress experimental values (σ^{Exp}) and the numerically obtained stress using the Prony Series (σ^{Prony}) for a given pair of strain rate ($\dot{\varepsilon}$) and temperature (T) is illustrated in Figure 2.

From now on, a set of experimental data is considered in which, for each temperature T_j, traction tests with different strain rates $\dot{\varepsilon}_i$ were performed. In this case, the total number of temperatures is denoted by *NTemp*, the total number of strain rates by *NSr* and the total number of sampled points from each curve by *NPt*. Thus, the absolute error, measured in stress and associated to the *k-th* point t_k $(1 \leq k \leq NPt)$, sampled for the *j-th* temperature T_j $(1 \leq j \leq NTemp)$ and the *i-th* strain rate $\dot{\varepsilon}_i$ $(1 \leq i \leq NSr)$, D_{kij} (Figure 2) can be obtained as

$$D_{kij} = D_{kij}\left(E_{\infty}, E_q, \dot{\varepsilon}_i, T_j, t_k\right) = \left|\sigma^{Exp}\left(\dot{\varepsilon}_i, T_j, t_k\right) - \sigma^{Prony}\left(E_{\infty}, E_q, \dot{\varepsilon}_i, T_j, t_k\right)\right|. \tag{8}$$

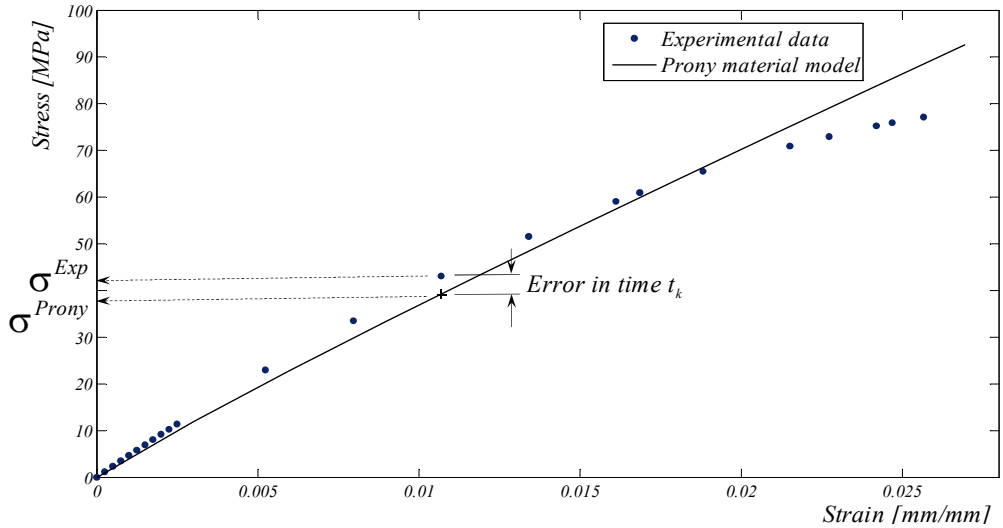

Figure 2: Experimental and Prony tensile versus strain for a determined strain rate.

Note that the σ_k^{Prony} stress is evaluated according to the constitutive Prony model by the hereditary integral (Eq. (7)), and σ_k^{exp} is the measured experimental stress, both obtained on the *k-th* point sampled. The symbol | | represents the absolute value of the function.

A measurement of the total error associated to the model can be obtained by the total quadratic error D_T^2, given by

$$D_T^2 = D_T^2\left(E_\infty, E_q\right) = \sum_{j=1}^{NTemp}\sum_{i=1}^{NSr}\sum_{k=1}^{NPt}\left[D_{kij}\left(E_\infty, E_q, \dot{\varepsilon}_i, T_j, t_k\right)\right]^2, \tag{9}$$

or by the average quadratic error ($\bar{D}_T$) defined as

$$\bar{D}_T = \frac{D_T^2}{\text{Total number of points}}. \tag{10}$$

This scalar function will be used as an objective function in the optimization process for the identification of the mechanical properties of the VME.

The following section presents the formulation for determining the influence of temperature and pressure on mechanical behavior.

2.3 Temperature Influence on Mechanical Behavior

In order to determinate the influence of temperature on mechanical behavior, the constitutive VEM model is used in association with parameter α_T. In this case, the relaxation modulus function could be written as

$$E(t) = E_{\infty} + \sum_{q=1}^{TN} E_q e^{\frac{-t}{\alpha_T \tau_q}}, \tag{11}$$

and the temperature shift factor α_T can be obtained by Williams, Landel and Ferry's model – the WLF model – (Williams et al., 1955) as

$$\log(\alpha_T) = \frac{-C_1(T - T_s)}{C_2 + (T - T_s)}. \tag{12}$$

In this model, T is the temperature in which the material's response is measured, T_s is the reference temperature, C_1 and C_2 are characteristics material properties, and α_T is the shift factor of all relaxation times. Thus, the convolution integral can be defined as

$$\sigma^{Prony}(t) = \sigma^{Prony}(E_{\infty}, E_i, t) = \int_0^t \left(E_{\infty} + \sum_{q=1}^{TN} E_q \, . e^{\frac{-(t-\tau)}{\alpha_T(T)\tau_q}} \right) \frac{d\varepsilon}{d\tau} d\tau \, . \tag{13}$$

In order to obtain the expression for the stress in the *k-th* time instant (t_k), in *i-th* temperature (T_i), and for the *j-th* strain rate ($\dot{\varepsilon}_j$), the Prony stress expression yields

$$\sigma^{Prony}(\dot{\varepsilon}_j, T_i, t_k) = \sigma^{Prony}(E_{\infty}, E_i, \dot{\varepsilon}_j, T_i, t_k) = E_{\infty} \, \dot{\varepsilon}_j \, t_k + \sum_{q=1}^{TN} E_q \, \dot{\varepsilon}_j \, I_{kiq} \, . \tag{14}$$

In this case, the last term of the Equation can be analytically obtained as

$$I_{kiq} = \int_0^{t_k} e^{\frac{-(t_k - \tau)}{\alpha_T(T_i)\tau_q}} d\tau = \alpha_T \tau_q \left(1 - e^{\frac{-t_k}{\alpha_T(T_i)\tau_q}} \right), \tag{15}$$

and the stress value in time t_k is given by

$$\sigma_{jik}^{Prony} = \sigma^{Prony}(\dot{\varepsilon}_j, T_i, t_k) = E_{\infty} \, \dot{\varepsilon}_j \, t_k + \sum_{q=1}^{TN} E_q \, \dot{\varepsilon}_j \, \alpha_T(T_i) \tau_q \left(1 - e^{\frac{-t_k}{\alpha_T(T_i)\tau_q}} \right), \tag{16}$$

After having calculated the Prony stress values at each point, one proceeds by evaluating the error on the *k-th* point resulting from the comparison with the experimental value. The latter yields the average quadratic error obtained for the entire curve set (Eq. 10).

2.4 Average Pressure Influence on Material Behavior

In order to consider the average hydrostatic pressure influence - arising from the stress field - a transformation of the relaxation modulus function along time is used in a similar way to the influence due to temperature (Tschoegl, 1989). In this case, considering a reference pressure value P_0, in

which the relaxation modulus $E(P_0;t')$ is defined, the material response for a given pressure is translated as

$$E\left(P_0;t'\right) = E\left(P;t = \alpha_P t'\right). \tag{17}$$

Thereby, considering the influence of hydrostatic pressure on instant t, the relaxation modulus expression could be written as

$$E\left(t\right) = E_\infty + \sum_{q=1}^{TN} E_q \, e^{\frac{-t}{\alpha_P \tau_q}}. \tag{18}$$

Here, the pressure shift factor (α_P) considered in the present work was proposed by O'Reilly (1962) as

$$\log\left(\alpha_P\right) = C\left(P - P_0\right), \tag{19}$$

where C is a constant characteristic of the material. Substituting the relaxation modulus expression $E(t)$, Eq. (18), in the convolution integral, Eq. (6) yields the stress in a given instant t as

$$\sigma^{Prony}(t) = \sigma^{Prony}\left(E_\infty, E_q\right) = E_\infty \, \dot{\varepsilon} \, t + \dot{\varepsilon} \sum_{q=1}^{TN} E_q \int_0^t e^{\frac{-(t-\tau)}{\alpha_P \tau_q}} \, d\tau \, . \tag{20}$$

It is possible to observe that, during load application process, the uniaxial stress is variable and therefore the translation generated by factor α_P is not constant (this is the opposite of the translation process due to temperature influence, α_T). In order to overcome this difficulty, the total integration interval is divided according to sampled points (Figure 3) and considered a constant value for the pressure P in each of these intervals. In this case, the *p-th* interval is defined by their lower (t_{p-1}) and upper limit values (t_p). The constant pressure value in this interval is denoted P_{jp}, Thus, it is possible to find the expression for the stress on the *k-th* instant of time (t_k) and for the curve associated to the *j-th* strain rate ($\dot{\varepsilon}_j$) as follows

$$\sigma_{jk}^{Prony} = \sigma^{Prony}\left(\dot{\varepsilon}_j, t_k\right) = E_\infty \, \dot{\varepsilon}_j \, t_k + \sum_{q=1}^{TN} E_q \, \dot{\varepsilon}_j \sum_{p=1}^{k} I_{pkq} \, , \tag{21}$$

such that

$$I_{pkq} = \int_{t_{p-1}}^{t_p} e^{-\left(\frac{t_k - \tau}{\alpha_P \tau_q}\right)} d\tau \cong \int_{t_{p-1}}^{t_p} e^{-\left(\frac{t_k - \tau}{\bar{\alpha}_P \tau_q}\right)} d\tau \, , \tag{22}$$

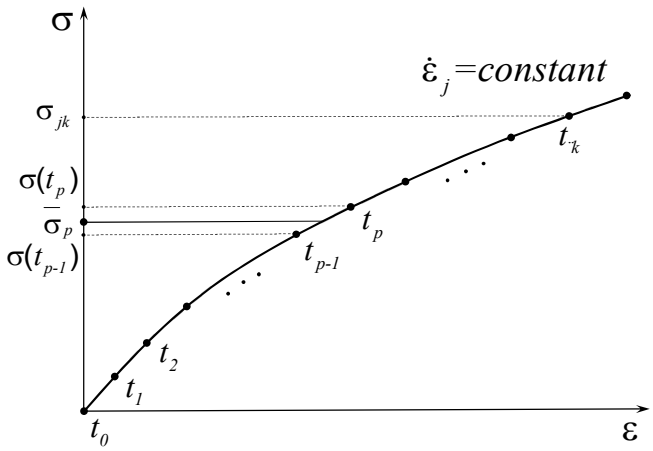

Figure 3: Integration interval division.

Note that, in Eq. (21), the first term corresponds to a purely elastic response between initial instant t_0 and final instant t_k. Thus, the second term represents the sum of all Prony Series terms $(1 \leq q \leq TN)$ throughout time (from *0* to t_k), but considering a discretization upon it. As the pressure is considered as constant in the interval from t_{p-1} to t_p $(1 \leq p \leq k)$, the same occurs for shift factor α_P. In that case, this parameter is denoted by $\bar{\alpha}_P = 10^{C\,(P_{jp}-P_0)}$, where P_{jp} is the average pressure in the interval $t_{p-1} \leq t \leq t_p$ and defined as $P_{jp} = -\overline{\sigma}_p/3$, where $\overline{\sigma}_p$ is the value of the average tension in that interval. So, the second term in Eq. (21), and therefore Eq. (22), - the term I_{pkq} - can be analytically solved considering a transformation of variables in the following form

$$-\left(\frac{t_k-\tau}{\overline{\alpha}_P\tau_q}\right)=\left(\frac{\tau-t_k}{\overline{\alpha}_P\tau_q}\right)=u\,. \tag{23}$$

Replacing this expression in (22) by I_{pkq}, the result is

$$I_{pkq}\cong\overline{\alpha}_P\,\tau_q\,e^{\left(\frac{t_{p-1}-t_k}{\overline{\alpha}_P\,\tau_q}\right)}\left[e^{\left(\frac{t_p-t_{p-1}}{\overline{\alpha}_P\,\tau_q}\right)}-1\right]. \tag{24}$$

Thus, the resulting expression for the stress value by the Wiechert model is

$$\sigma^{Prony}\left(\dot{\varepsilon}_j,t_k\right)=E_\infty\,\dot{\varepsilon}_j\,t_k+\sum_{p=1}^{k}\sum_{q=1}^{TN}\dot{\varepsilon}_j\,\overline{\alpha}_P\,E_q\,\tau_q\,e^{\left(\frac{t_{p-1}-t_k}{\overline{\alpha}_P\,\tau_q}\right)}\left[e^{\left(\frac{t_p-t_{p-1}}{\overline{\alpha}_P\,\tau_q}\right)}-1\right]. \tag{25}$$

Inserting the value obtained from Eq. (25) into Eq. (10) yields the average quadratic error obtained for the entire curve set.

2.5 Optimization Process

The present work has studied the influence of two variables in an independent way upon material behavior, temperature, and hydrostatic pressure. In the first case, the material properties referring to the influence of average pressure on the material at a constant temperature could be obtained by the solution of the following optimization problem:

$$\begin{aligned} &Minimize\ \bar{D}_T\left(\boldsymbol{x}\right) : \Re^{TN+4} \rightarrow \Re \\ &where\ \boldsymbol{x} = \left\{E_\infty,\ E_i,\ C_1,\ C_2,\ T_s\right\}\ \left(i = 1,...TN\right)\ . \\ &Constraints: \begin{cases} 0 \leq E_\infty \leq E_\infty^{upp} \\ 0 \leq E_i \leq E_i^{upp}\ \left(i = 1,...TN\right) \\ C_1^{low} \leq C_1 \leq {C_1}^{upp} \\ C_2^{low} \leq C_2 \leq {C_2}^{upp} \\ T_s^{low} \leq T_S \leq {T_S}^{upp} \end{cases} \end{aligned} \tag{26}$$

where E_∞^{upp}, E_i^{upp}, C_1^{low}, ${C_1}^{upp}$, C_2^{low}, ${C_2}^{upp}$, T_s^{low} and ${T_S}^{upp}$ are arbitrated values of the upper and lower limits of components of the design variables $\boldsymbol{x}$. In this standard optimization problem, the goal is to minimize error $\bar{D}_T$, with design variables being: equilibrium modulus E_∞, relaxation modulus E_i, material constants C_1 and C_2, and reference temperature T_s.

In the second case, to consider solely the influence of the pressure shift factor, the optimization standard problem is defined as follows:

$$\begin{aligned} &Minimize\ \bar{D}_T\left(\boldsymbol{x}\right) : \Re^{TN+3} \rightarrow \Re \\ &where\ \boldsymbol{x} = \left\{E_\infty,\ E_i,\ C,\ P_0\right\}\ \left(i = 1,...TN\right)\ . \\ &Constraints: \begin{cases} 0 \leq E_\infty \leq E_\infty^{upp} \\ 0 \leq E_i \leq E_i^{upp}\ \left(i = 1,...TN\right) \\ C^{low} \leq C \leq C^{upp} \\ P_0^{low} \leq P_0 \leq {P_0}^{upp} \end{cases} \end{aligned} \tag{27}$$

In that case, E_∞^{upp}, E_i^{upp}, C^{low}, C^{upp}, P_0^{low} and P_0^{upp} are arbitrated values which represent the upper and lower limits of design variables $\boldsymbol{x}$. In this standard problem, similarly to the temperature case, the objective is to minimize error $\bar{D}_T$, and the design variables are: equilibrium modulus E_∞, relaxation modulus components set E_i, material constant C and reference pressure P_0.

3 NUMERICAL RESULTS

3.1 VEM Experimental Analysis

The experiments were supplied by material manufacturer SABIC, and were realized on material Stamax 30YM240, with 30% concentration of long fiber glass, in accordance with norm ISO 527/1B

(ISO, 2012). According to SABIC, the material was submitted to three sets of tests of pure traction, each one at a different and constant temperature (-35ºC, 23ºC, and 80ºC). In each of those temperatures, that material has been submitted to four different strain rates, constant throughout each particular test (0.0001(mm/mm)/s, 0.01(mm/mm)/s, 0.1(mm/mm)/s, and 1(mm/mm)/s). By performing these tests, it was possible for supplier SABIC to obtain tensile and strain experimental data for each strain rate and temperature. Those experimental data are shown in the appendix, and compose the entry file for the identification process in the shape of an inverse problem, whose codes were implemented on MATLAB software.

3.2 Implemented Computational Structure

The flowchart of the implemented computational structure is shown in Figure 4. First step is the reading of data from experimental tests, followed by the preparation of GA routine and its execution. Then, the best point obtained from the optimization process using GA serves as entry data for the preparation of the nonlinear programming routine and its execution. The final result reaches the global optimum point. Finally, results are displayed. In this optimization process, the MATLAB: GA (for genetic algorithm) and the FMINCON (for nonlinear programming) toolboxes were used.

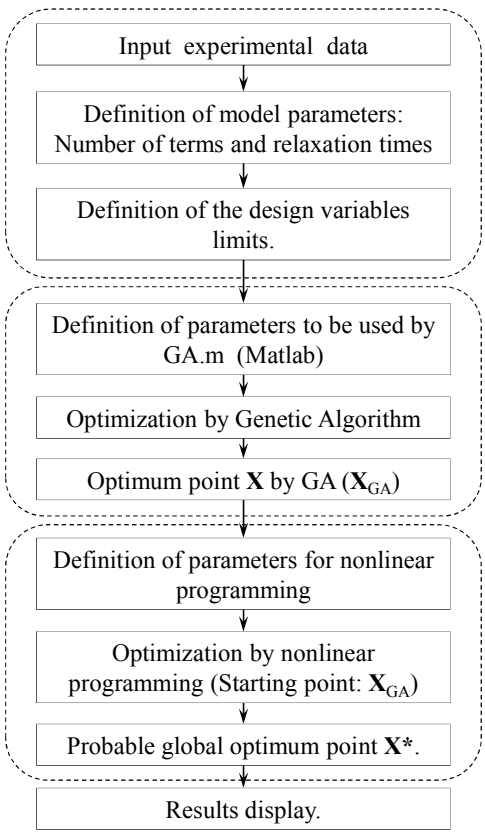

Figure 4: Scheme of routine set implemented on MATLAB software for material characterization.

3.3 Identification of VEM Considering Influence of Pressure and Constant Temperature

The results presented in this section consider the material model with one spring term according to Figure 1, or Wiechert model, which contains one term representing pure elastic behavior. Therefore, the objective is to obtain the minimum error resulting from a comparison between experimental data and the data obtained from Prony Series implementation, and analyzing the influence of pressure, with constant temperature. In all following analysis performed and presented, some parameters of the optimization process are common and named in Table 1.

In the numerical identification process, the relaxation times were arbitrated as $\tau = \{0.010000; 0.071969; 0.517947; 3.727594; 26.82696; 193.069773; 1389.495494; 10000.000000\}$ and the range of reference pressure was also arbitrated in the interval from $-3 \cdot P_{med}$ to P_{med} in order to impress more flexibility to the adjustment, and P_{med} is equivalent to one third of the maximum tensile of the curve.

Coefficient	Symbol	Value
GA - Population		200
GA - Generations		200
GA – Function Tolerance	TolFun	1e-6
GA - Mutations	MutationFcn	@mutationadaptfeasible,0.02
NLP	MaxFunEvals	100
NLP	MaxIter	400
NLP Algorithm	Active-set	
Equilibrium Modulus	E_∞	$0 \text{ MPa} \leq E_\infty \leq 10000 \text{ MPa}$
Prony Series components	E_i (i = 1...TN) (TN = 8)	$0.0 \text{ MPa} \leq E_i \leq 5000 \text{ MPa}$
OR – Material constant	C	$-0.4 \leq C \leq 0.4$
OR – Reference pressure	P_0	$-3*P_{med} \leq P_0 \leq P_{med}$

Table 1: Coefficients used on pressure influence analysis.

3.4 Identification Considering the Influence of Pressure at -35°C Constant Temperature

This section presents the results obtained for the constant temperature of -35ºC, and a comparison between experimental data and data obtained through Prony Series calculation. The results contemplate the comparison focusing on each of the strain rates separately, for a fixed temperature of -35ºC.

Analyzing the results in Table 2, one can observe that the strain rate applied in the experimental test has a strong influence over the constants that characterize the relaxation modulus behavior and over the reference pressure P_0, which significantly present different values for each strain rate. In another way, the value of constant C_0 presented quite a low value for all the strain rates. It can also be observed that the equilibrium modulus showed values different from zero for all strain rates. Inserting the values obtained in Table 2 into Eq. (18) yields the relaxation modulus function, which can be visualized in Figure 6.

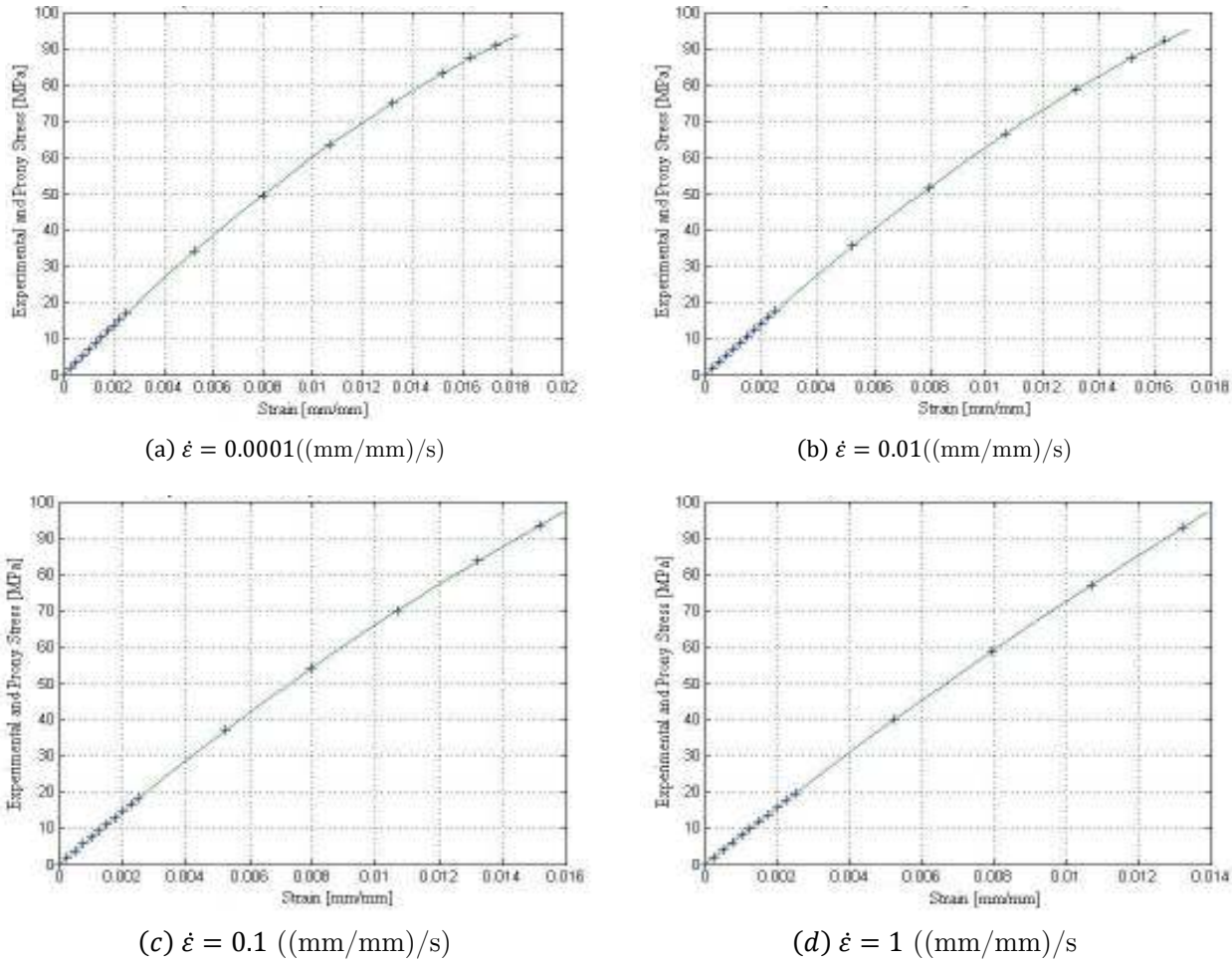

(a) $\dot{\varepsilon} = 0.0001((\mathrm{mm/mm})/\mathrm{s})$ (b) $\dot{\varepsilon} = 0.01((\mathrm{mm/mm})/\mathrm{s})$

$(c)\ \dot{\varepsilon} = 0.1\ ((\mathrm{mm/mm})/\mathrm{s})$ $(d)\ \dot{\varepsilon} = 1\ ((\mathrm{mm/mm})/\mathrm{s}$

Figure 5: Comparison between experimental tensile results (+) and the values obtained from Prony model (—) for -35°C temperature and four single strain rates.

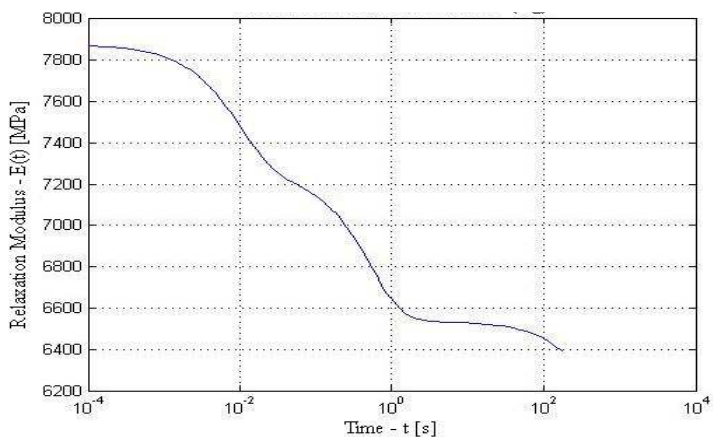

Figure 6: Relaxation modulus function identified considering strain rates and -35°C temperature.

	Strain rate ((mm/mm)/s)		$\dot{\varepsilon}$= 0.0001	$\dot{\varepsilon}$= 0.01	$\dot{\varepsilon}$= 0.1	$\dot{\varepsilon}$=1	Global adjustment
τ_1 (s)	0.010000	E_1 (MPa)	1009.1	713.8	499.0	205.4	595.2
τ_2 (s)	0.071960	E_2 (MPa)	206.2	259.8	149.7	11.5	0.0
τ_3 (s)	0.517896	E_3 (MPa)	0.0	0.0	0.0	146.0	739.3
τ_4 (s)	3.727297	E_4 (MPa)	0.0	121.2	155.2	78.8	0.0
τ_5 (s)	26.825356	E_5 (MPa)	187.6	368.7	323.6	355.2	0.0
τ_6 (s)	193.062086	E_6 (MPa)	825.6	500.9	406.1	57.6	0.0
τ_7 (s)	1389.467834	E_7 (MPa)	3189.2	554.4	435.9	92.7	1139.5
τ_8 (s)	10000.000000	E_8 (MPa)	1856.7	1094.3	806.9	622.2	448.0
	E_∞ (MPa)		1045.6	4646.0	5373.7	6574.6	4947.3
	C		0.4	0.4	0.4	0.4	0.4
	P_0 (MPa)		11.6369	14.9452	20.3969	10.5366	-4.8053
	GA Error (MPa^2)		0.0298	2.1177	0.7736	0.5757	2.9194
	Minimum error (MPa^2)		2.1678E-04	3.4934E-05	1.9042E-05	2.9437E-06	1.1756

Table 2: Results of the identification process for -35°C temperature.

3.5 Identification Considering Only the Influence of Temperature

The results presented in the subsequent sections also consider the Wiechert model, which contains one term representing pure elastic behavior. In this case, the minimum error is obtained as a result of the comparison between experimental data and the data obtained from the implementation of the model based on Prony Series, now analyzing the influence of temperature. It can be said that those results do not consider the influence of average pressure on the model point. In the following analysis, performed and presented, the optimization process parameters for GA and NLP and the relaxation times are shown in Table 3.

Coefficient	Symbol	Value
WLF – Material constant 1	C_1	$-10.0 \leq C_1 \leq 10.0$
WLF – Material constant 2	C_2	$-200.0^{o}\,C \leq C_2 \leq 200.0^{o}\,C$
WLF – Reference temperature	T_s	$-90.0^{o}\,C \leq T_s \leq 90.0^{o}\,C$

Table 3: Coefficients used in the analysis of temperature influence.

3.5.1 Identification considering strain rate 1 ((mm/mm)/s) and temperatures of -35°C, 23°C, and 80°C

This section presents the results for temperatures of -35°C, 23°C, and 80°C, comparing experimental data and the data obtained from the calculation of Prony Series for the strain rate of 1.0 (mm/mm)/s. Figure 8 presents the relaxation modulus function for the reference temperature of -55.46°C, obtained by inserting the values from Table 4 into Eq. (11). Analyzing the results in Table 4, it becomes clear that the influence is not only that of temperature, but also of the strain rate applied to the load on the material test, with variation on the equilibrium modulus values and on the constants related to each component of the series.

3.5.2 Identification Considering all Strain Rates and Temperatures

This section presents the results for temperatures of -35°C, 23°C, and 80°C comparing experimental data and the data obtained from Prony Series calculation for all strain rates presented before (Figure 7).

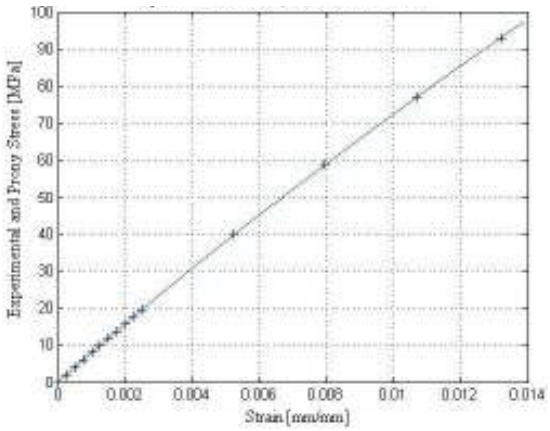

(a) T = -35°C.

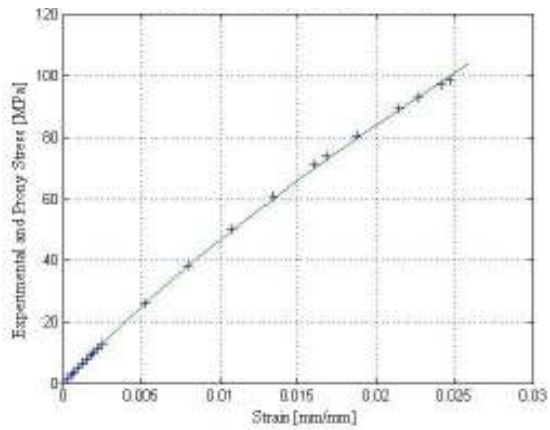

(b) T = 23°C.

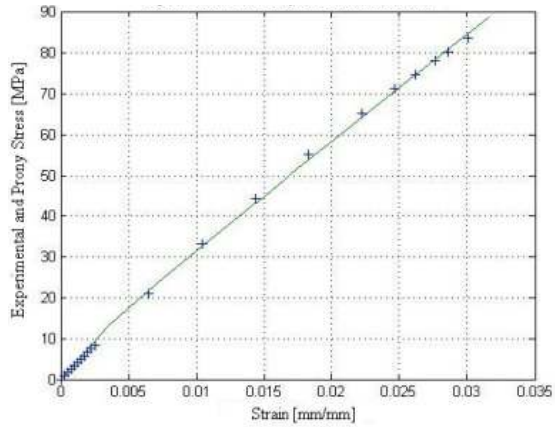

(c) T = 80°C.

Figure 7: Comparison between experimental tensile results and those obtained from Prony Series for temperatures of -35°C, 23°C, and 80°C, and strain rate of 1.0 (mm/mm)/s.

The results presented in Table 5 used the Wiechert model, obtaining equilibrium modulus greater than zero. This shows the influence of pure elastic behavior on the VEM behavior. One could also assure the influence of temperature by the variation of constants C_1, C_2, and reference temperature T_s, which are parameters used in the calculation of temperature shift factor, a_T.

Inserting the values obtained in Table 5 into Eq. (11) yields the relaxation modulus function. This function can be visualized in Figure 9, and it considers the history of all temperatures and strain rates, constituting the master curve for reference temperature of, approximately, -18.38°C, obtained through the optimization process.

Identification Process Results for Strain Rate $\dot{\varepsilon}$= 1 ((mm/mm)/s)			
Relaxation time (s)		Relaxation Modulus	
τ_1 (s)	0.010000	E_1 (MPa)	0.0
τ_2 (s)	0.071960	E_2 (MPa)	0.0
τ_3 (s)	0.517896	E_3 (MPa)	2524.9
τ_4 (s)	3.727297	E_4 (MPa)	0.0
τ_5 (s)	26.825356	E_5 (MPa)	0.0
τ_6 (s)	193.062086	E_6 (MPa)	2301.1
τ_7 (s)	1389.467834	E_7 (MPa)	0.0
τ_8 (s)	10000.000000	E_8 (MPa)	1021.0
E_∞ (MPa)		2217.5	
C_1	10.0	C_2 (°C)	103.8183
T_s (°C)		-55.4621	
GA Error (MPa^2)		0.6899	
Minimum error (MPa^2)		0.3051	

Table 4: Results of the identification process for temperatures of -35°C, 23°C, and 80°C, and strain rate of1.0 (mm/mm)/s.

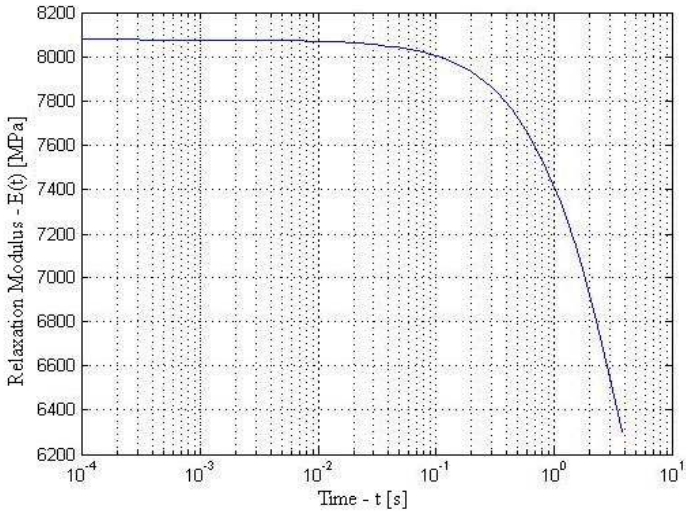

Figure 8: Relaxation modulus function identified considering strain rate of 1.0 (mm/mm)/s and temperatures of -35°C, 23°C, and 80°C.

The glass transition temperature of the analyzed material is 0°C, but in the researched literature different options were adopted for the reference temperature of the temperature shift factor WLF, which is the model adopted in the present work. After performing tests with different options of reference temperature T_s, - from glass transition temperature to 50°C above it - it was decided that this could be consider a free parameter, with boundaries between +/- 90°C.

Identification Process Results			
Relaxation time (s)		Relaxation Modulus	
τ_1 (s)	0.010000	E_1 (MPa)	992.7
τ_2 (s)	0.071960	E_2 (MPa)	0.0
τ_3 (s)	0.517896	E_3 (MPa)	0.0
τ_4 (s)	3.727297	E_4 (MPa)	1911.5
τ_5 (s)	26.825356	E_5 (MPa)	233.7
τ_6 (s)	193.062086	E_6 (MPa)	0.0
τ_7 (s)	1389.467834	E_7 (MPa)	1228.9
τ_8 (s)	10000.000000	E_8 (MPa)	0.0
E_∞ (MPa)			2369.4
C_1			10.0
C_2 (ºC)			101.1856
T_s (ºC)			-18.38
GA Error (MPa^2)			22.2881
Minimum error (MPa^2)			21.2534

Table 5: Results from identification process for all temperatures (-35°C, 23°C, and 80°C) and all strain rates (0.0001, 0.01, 0.1, and 1.0 (mm/mm)/s).

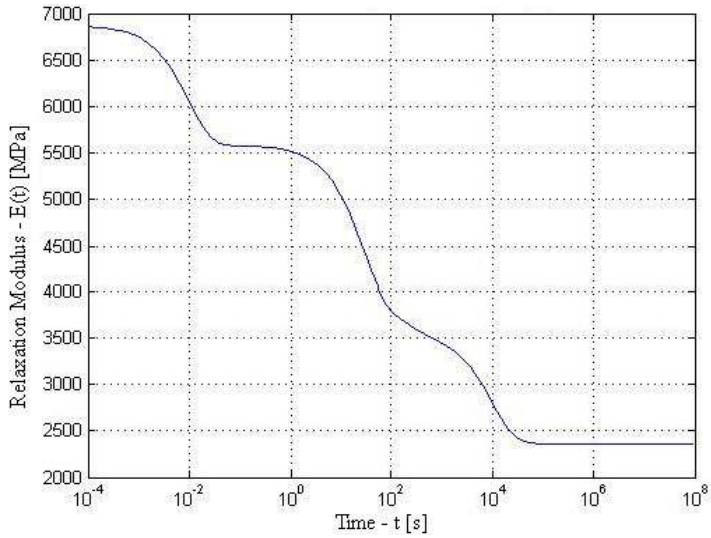

Figure 9: Relaxation modulus function identified considering all strain rates and temperatures for $T_s =$ -18.38°C.

4 CONCLUSIONS

The present work proposes a methodology for VEM characterization through an inverse identification problem in the time domain. The methodology developed permits to characterize viscoelastic materials with a thermorheologically and piezorheologically simple behavior. For this purpose, experimental data, extracted from tensile versus strain curves - in different strain rates and temperatures - were used as a starting point.

The implemented formulation was based on the constitutive model of Prony Series. The inverse identification process used a hybrid optimization technique (GA and NLP) implemented in MATLAB.

The following simulations were performed:

a) Influence of pressure
Case 1 – A single strain rate for a single temperature;
Case 2 – Several strain rates for a single temperature;

b) Influence of temperature
Case 3 – A single strain rate for several temperatures;
Case 4 – Several strain rates for several temperatures.

In case 1, where the curves are adjusted individually, the final quadratic errors ranged from 10^{-04} MPa^2 to 10^{-06} MPa^2, which indicates that the constitutive model used could be adequate for the material under study, and the methodology adopted proved to be efficient for the identification of mechanical properties. For case 2, where several curves are adjusted for a single temperature, the

errors ranged from 1 MPa^2 to 4 MPa^2. This increase in average error resulting from the adjustment can be attributed to the fact that the chosen model for evaluating the influence of pressure is linear.

In case 3, where several temperatures are adjusted for the same strain rate, the errors can be considered as low value errors, but higher than the ones in case 1. This can be attributed to the fact that the influence of pressure was not considered, but only the influence of temperature. At last, in case 4 - where a global adjustment occurs - considering all strain rates and temperatures available, the error was around 21 MPa^2. Despite being higher when compared to the errors found in the other cases, it can still be considered satisfactory, because it represents an average error of around 5% in each sampled point.

The results show that the implemented methodology can be considered adequate for characterizing viscoelastic materials in the time domain, provided that they have a behavior similar to that of the hypothesis considered, although better results can be obtained by using more precise models that are able to take into consideration the influence of pressure, the influence of temperature, and a combined influence of pressure and temperature. It must be stated that it may also be the case that the investigated material is not thermorheologically and piezorheologically simple, and a study aiming at confirming such statement could be developed in the future.

References

Bagley, R. L., Torvik, P. J. (1983). A theoretical basis for the application of fractional calculus to viscoelasticity. Journal of Rheology, 27(3): 201-210.

Beake, B. (2006). Modelling indentation creep of polymers: a phenomenological approach. Journal of Physics D: Applied Physics, 39: 4478-4485.

Brinson, H. L., Brinson, L. C. (2008). Polymer Engineering Science and Viscoelasticity, Springer Verlag (New York).

Chae, S.-H., Zhao, J.-H., Edwards, D. R., Ho P. S. (2010). Characterization of the viscoelasticity of molding compounds in the time domain. Journal of Electronic Materials, 39(4): 419-425.

Chen, T. (2000). Determining a Prony Series for a viscoelastic material from time varying strain data. Internal report. NASA - National Technical Information Service.

Christensen, R. M. (1971). Theory of Viscoelasticity. Academic Press (New York).

Felhös, D., XU, D., Schlare, A. K., Váradi, K., Goda T. (2008). Viscoelastic characterization of an EPDM rubber and finite element simulation of its dry rolling friction. eXPRESS Polymer Letters, 2(3): 157-164.

Ferry, J. D. (1980). Viscoelastic Properties of Polymers. John Wiley & Sons (New York).

Flügge, W. (1975). Viscoelasticity. Springer Verlag (New York).

Hu, G., Tay, A. A. O., Zhang Y., Zhu, W., Chew, S. (2006). Characterization of viscoelastic behaviour of a molding compound with application to delamination analysis in IC packages. Electronics Packaging Technology Conference, 53-59.

Huang, G., Wang, B., Lu, H. (2004). Measurements of viscoelastic functions of polymers in the frequency-domain using nanoindentation. Mechanics of Time-Dependent Materials, 8(4): 345-364.

Iso 527/1B (2012). Plastics – Determination of tensile properties. International Organization Standardization, Geneva (Switzerland).

Leaderman, H. (1943). Elastic and Creep Properties of Filamentous Materials and Other High Polymers. Washington, D. C.: The Textile Foundation.

Li, Z.-D., Liu, H.-J., Zhang, R.-F., Yi, H. (2007). Time-temperature-stress superposition principle of PMMA's crazing damages under creep condition. Journal of Central South University of Technology, 14: 318-323.

Lima, A.M.G., Stoppa, M.H., Rade, D.A. (2004). Finite element modeling and experimental characterization of beams and plates treated with constraining damping layers. ABCM Symposium Series in Mechatronics, 1: 311-320.

Lopes, E. M. O., Bavastri, C. A., Neto, J. M. S., Espíndola, J. J. (2004). Caracterização dinâmica integrada de elastômeros por derivadas generalizadas. In the III Congresso Nacional de Engenharia Mecânica (CONEM), Belém, Brasil.

Mainardi, F. (2010). Fractional Calculus and Waves in Linear Viscoelasticity - An Introduction to Mathematical Models. Imperial College Press (London).

O'Reilly, J. M. (1962). The effect of pressure on glass temperature and dielectric relaxation time of polyvinyl acetate. Journal of Polymer Science, 57: 429-444.

Pacheco, J. E. L.(2013). Caracterização de Materiais Viscoelásticos com Aplicação de Séries de Prony e Análise por Elementos Finitos, M.Sc. Dissertation (in Portuguese), Federal University of Paraná, Brasil.

Park, S. W., Schapery, R. A. (1999). Methods of interconversion between linear viscoelastic material functions. Part I – a numerical method based on Prony Series. International Journal of Solids and Structures, 36: 1653-1675.

Pritz, T. (1996). Analysis of four-parameter fractional derivative model of real solid materials. Journal of Sound and Vibration, 195: 103-115.

Schwarzl, F., Staverman, A. J. (1952). Time temperature dependence of linear viscoelastic behavior. Journal of Applied Physics, 23: 838.

Sorvari, J., Hämäläinen, J. (2010). Time integration in linear viscoelasticity – a comparative study. Mechanics of Time-Dependent Materials, 14(3): 307-328.

Sorvari, J., Malinen, M. (2007). On the direct estimation of creep and relaxation functions. Mechanics of Time-Dependent Materials, 11(2): 143-157.

Tobolsky, A. V. (1956). Stress relaxation studies of the viscoelastic properties of polymers. Journal of Applied Physics, 27: 673.

Tschoegl, N. W. (1989). The Phenomenological Theory of Linear Viscoelastic Behavior. Springer Verlag (Berlim).

Tschoegl, N. W., Knauss, W. G., Emri, I. (2002). The effect of temperature and pressure on the mechanical properties of thermo- and/or piezorheologically simple polymeric materials in thermodynamic equilibrium – a critical review. Mechanics of Time-Dependent Materials, 6: 53-99.

Williams, M. L., Landel, R. F., Ferry, J. D. (1955). The temperature dependence of relaxation mechanisms in amorphous polymers and other glass-forming liquids. Journal of the American Chemical Society, 77 (14): 3701-3706.

APPENDIX

Appendix 1 – Data from experimental testing for all strain rates and temperatures of -35ºC, 23ºC and 80ºC

In this section experimental data provided by supplier of material STAMAX are presented for strain rates of 0.0001, 0.01, 0.1 and 1 (mm/mm)/s and temperatures of -35ºC, 23ºC and 80ºC.

Strain rate: 0.0001 (mm/mm)/s		Strain rate: 0.01 (mm/mm)/s	
Strain (mm/mm)	Stress (MPa)	Strain (mm/mm)	Stress (MPa)
0.000000	0.000000	0.000000	0.000000
0.000250	1.757970	0.000250	1.814182
0.000500	3.502835	0.000500	3.615712
0.000750	5.234583	0.000750	5.404579
0.001000	6.953206	0.001000	7.180774
0.001249	8.658691	0.001249	8.944286
0.001499	10.351029	0.001499	10.695105
0.001748	12.030210	0.001748	12.433220
0.001998	13.696222	0.001998	14.158623
0.002247	15.349055	0.002247	15.871302
0.002497	16.988700	0.002497	17.571247
0.005236	34.151298	0.005236	35.427315
0.007968	49.702776	0.007968	51.727852
0.010693	63.629183	0.010693	66.459329
0.013212	75.078506	0.013212	78.705590
0.015184	83.065019	0.015184	87.351327
0.016365	87.435287	0.016365	92.131625
0.017349	90.834579	- - -	- - -

Table 6: Experimental data for temperatures -35°C and strain rates 0.0001 and 0.01 (mm/mm)/s.

Strain rate: 0.1 (mm/mm)/s		Strain rate: 1.0 (mm/mm)/s	
Strain (mm/mm)	Stress (MPa)	Strain (mm/mm)	Stress (MPa)
0.000000	0.000000	0.000000	0.000000
0.000250	1.870858	0.000250	1.987724
0.000500	3.730444	0.000500	3.966243
0.000750	5.578749	0.000750	5.935549
0.001000	7.415763	0.001000	7.895636
0.001249	9.241478	0.001249	9.846495
0.001499	11.055894	0.001499	11.788118
0.001748	12.858974	0.001748	13.720499
0.001998	14.650736	0.001998	15.643628
0.002247	16.431162	0.002247	17.557500
0.002497	18.200243	0.002497	19.462106
0.005236	36.908734	0.005236	39.799030
0.007968	54.231174	0.007968	59.003677
0.010693	70.155383	0.010693	77.065871
0.013410	83.661453	0.013410	92.784735
0.015184	93.399564	0.015184	87.351327
- - -	- - -	0.016365	92.131624

Table 7: Experimental data for temperatures -35°C and strain rates 0.1 and 1.0 (mm/mm)/s.

Strain rate: 0.0001 (mm/mm)/s		Strain rate: 0.01 (mm/mm)/s	
Strain (mm/mm)	Stress (MPa)	Strain (mm/mm)	Stress (MPa)
0.000000	0.000000	0.000000	0.0000000
0.000250	1.138259	0.000250	1.174656
0.000500	2.268033	0.000500	2.341120
0.000750	3.389315	0.000750	3.499385
0.001000	4.502098	0.001000	4.649445
0.001249	5.606374	0.001249	5.791293
0.001499	6.702138	0.001499	6.924922
0.001748	7.789383	0.001748	8.050326
0.001998	8.868101	0.001998	9.167498
0.002247	9.938286	0.002247	10.276432
0.002497	10.999931	0.002497	11.377122
0.005236	22.112459	0.005236	22.938662
0.007968	32.181811	0.007968	33.493018
0.010693	41.198953	0.010693	43.031430
0.013410	49.154851	0.013410	51.545140
0.016119	56.040471	0.016119	59.025388
0.016857	57.731429	0.016857	60.884942
0.018822	61.846778	0.018822	65.463413
0.021517	66.564739	0.021517	70.850457
0.022739	68.347039	0.022739	72.949312
0.024205	70.185319	0.024205	75.177759
0.024693	70.725000	0.024693	75.850000
- - -	- - -	0.025668	77.088305

Table 8: Experimental data for temperatures 23°C and strain rates 0.0001 and 0.01 (mm/mm)/s.

Strain rate: 0.1 (mm/mm)/s		Strain rate: 1.0 (mm/mm)/s	
Strain (mm/mm)	Stress (MPa)	Strain (mm/mm)	Stress (MPa)
0.000000	0.000000	0.000000	0.000000
0.000250	1.211353	0.000250	1.287022
0.000500	2.415407	0.000500	2.568083
0.000750	3.612157	0.000750	3.843180
0.001000	4.801597	0.001000	5.112307
0.001249	5.983720	0.001249	6.375459
0.001499	7.158522	0.001499	7.632632
0.001748	8.325995	0.001748	8.883819
0.001998	9.486134	0.001998	10.129018
0.002247	10.638934	0.002247	11.368221
0.002497	11.784387	0.002497	12.601425
0.005236	23.897858	0.005236	25.769282
0.007968	35.113882	0.007968	38.204006
0.010693	45.424571	0.010693	49.899009
0.013410	54.822039	0.013410	60.847702
0.016119	63.298402	0.016119	71.043497
0.016857	65.449238	0.016857	73.692634
0.018822	70.845771	0.018822	80.479805
0.021517	77.456262	0.021517	89.150038
0.022739	80.149186	0.022739	92.836022
0.024205	83.121988	0.024205	97.047607
0.024693	84.050000	0.024693	98.400000
0.025668	85.811357	- - -	- - -
0.026642	87.446174	- - -	- - -

Table 9: Experimental data for temperatures 23°C and strain rates 0.1 and 1.0 (mm/mm)/s.

Strain rate: 0.0001 (mm/mm)/s		Strain rate: 0.01 (mm/mm)/s	
Strain (mm/mm)	Stress (MPa)	Strain (mm/mm)	Stress (MPa)
0.000000	0.000000	0.000000	0.000000
0.000250	0.740421	0.000250	0.807246
0.000500	1.475680	0.000500	1.608983
0.000750	2.205773	0.000750	2.405205
0.001000	2.930697	0.001000	3.195909
0.001249	3.650447	0.001249	3.981089
0.001499	4.365019	0.001499	4.760741
0.001748	5.074409	0.001748	5.534862
0.001998	5.778612	0.001998	6.303445
0.002247	6.477625	0.002247	7.066488
0.002497	7.171444	0.002497	7.823986
0.006479	17.562684	0.006479	19.186152
0.010445	26.606053	0.010445	29.109403
0.014396	34.284568	0.014396	37.575581
0.018331	40.581244	0.018331	44.566529
0.022251	45.479096	0.022251	50.064090
0.024693	47.822366	0.024693	52.733637
0.026155	48.961139	0.026155	54.050106
- - -	- - -	0.027615	55.151462
- - -	- - -	0.028587	55.765718
- - -	- - -	0.030044	56.506422

Table 10: Experimental data for temperatures 80°C and strain rates 0.0001 and 0.01 (mm/mm)/s.

Strain rate: 0.1 (mm/mm)/s		Strain rate – 1.0 (mm/mm)/s	
Strain (mm/mm)	Stress (MPa)	Strain (mm/mm)	Stress (MPa)
0.000000	0.000000	0.000000	0.000000
0.000250	0.822801	0.000250	0.833062
0.000500	1.641201	0.000500	1.663745
0.000750	2.455197	0.000750	2.492049
0.001000	3.264786	0.001000	3.317970
0.001249	4.069963	0.001249	4.141507
0.001499	4.870725	0.001499	4.962658
0.001748	5.667068	0.001748	5.781420
0.001998	6.458989	0.001998	6.597791
0.002247	7.246485	0.002247	7.411770
0.002497	8.029551	0.002497	8.223354
0.006479	19.953262	0.006479	20.881299
0.010445	30.727342	0.010445	32.917063
0.014396	40.337018	0.014396	44.322065
0.018331	48.767515	0.018331	55.087725
0.022251	56.004057	0.022251	65.205464
0.024693	59.914027	0.024693	71.196215
0.026155	62.031871	0.026155	74.666700
0.027615	63.977660	0.027615	78.043658
0.028587	65.178882	0.028587	80.242781
0.030044	66.836181	0.030044	83.462854
0.031983	68.774905	- - -	- - -

Table 11: Experimental data for temperatures 80**°**C and strain rates 0.1 and 1.0 (mm/mm)/s.